VIBRATION ANALYSIS OF A SELF-EXCITED SYSTEM WITH PARAMETRIC FORCING AND NONLINEAR STIFFNESS

GRZEGORZ LITAK*, GRZEGORZ SPUZ-SZPOS,
KAZIMIERZ SZABELSKI and JERZY WARMIŃSKI
*Department of Mechanics, Technical University of Lublin,
Nadbystrzycka 36, Lublin 20–618, Poland*

Vibrations of a self-excited oscillator under parametric excitation with nonlinear stiffness were investigated in this paper. Differential equation of motion includes van der Pol, Mathieu and Duffing terms. Vibrations synchronization, stability of solutions were examined by means of the multiple time scale method and Floquet theory. Chaotic solutions were found by means of Lyapunov exponent.

1. Introduction

In mechanical vibrations, we can distinguish a rather broad class of the self-excited systems with simultaneous parametric excitation [Szabelski, 1991]. In nonlinear systems there exists mutual interaction between these two types of vibrations which breaks the superposition rule. Numerous scientific monographs are concerned with the problems of synchronization (entrainment of frequency) in the self-excited system with parametric and external excitations [Szabelski & Warmiński, 1995a, 1995b]. The aim of this work is to analyze of the effects of interaction between self-excited and parametric vibrations of the main resonance and their effect on system transition to chaotic motion.

Let us examine vibrations of parametrically and self-excited systems described by differential equation [Szabelski, 1984; Huseyin & Rui, 1992; Rui & Huseyin, 1992]:

$$\ddot{x} - (\alpha_1 - \beta_1 x^2)\dot{x} + (\delta - \mu_1 \cos \Omega t)x + \gamma_1 x^3 = 0. \quad (1)$$

Our model possesses nonlinear van der Pol and Mathieu terms and parametric excitation of Duffing type. van der Pol systems with external forcing were intensively examined in the context of electric systems [van der Pol, 1926; Ueda & Akamatsu, 1981] and biological systems e.g. the heart model [van der Pol & van der Mark, 1928; von Hertzen & Kongas, 1996]. In our paper we discuss vibrations of van der Pol self-excited system with parametric forcing instead of external one. Most of real dynamic systems are affected by forces of nonlinear characteristics. In our system we assumed nonlinear term of Duffing type which can have both stiff and soft characteristics.

The article is organized as follows: After a short introduction (in Sec. 1) we analyze vibration in the vicinity of main resonance (Sec. 2) and obtain analytic forms of the solution. The comparison between analytic and numerical simulation results is also given. These results we use in the next, Sec. 3 where we provide the analysis of stability solution applying Floquet theory. Section 4 is concerned with numerical exploration of chaotic motion of the examined system. There we investigate chaotic motion using different methods. The Lyapunov exponent criterion is applied to find regions of parameters indicating chaotic behavior. Some examples of Poincaré maps, time histories and phase portraits

---

*E-mail: litak@archimedes.pol.lublin.pl

are plotted to illustrate the type and the evolutions of strange attractors. In Sec. 5 we end up with summary and conclusions.

2. Vibrations in Case of the Main Resonance

Introducing a small parameter $\varepsilon \ll 1$ into Eq. (1) we obtain:

$$\ddot{x} + \delta x = \varepsilon[(\alpha - \beta x^2)\dot{x} + \mu x \cos \Omega t - \gamma x^3], \quad (2)$$

where $\alpha\varepsilon = \alpha_1$, $\beta\varepsilon = \beta_1$, $\mu\varepsilon = \mu_1$ and $\gamma\varepsilon = \gamma_1$.

In case of the main parametric resonance for $\delta = 1$ ($\Omega \approx 2$), we can write:

$$\frac{1}{4}\Omega^2 \approx 1 + \varepsilon\sigma_1. \quad (3)$$

Applying this relation to (2), we get:

$$\ddot{x} + \frac{1}{4}\Omega^2 x = \varepsilon[(\alpha - \beta x^2)\dot{x} + \sigma_1 x + \mu x \cos \Omega t - \gamma x^3]. \quad (4)$$

To find an analytic solutions of Eq. (4) near the resonance we proceed the multiple time scale method [Szabelski *et al.*, 1996]:

$$\frac{d}{dt} = D_0 + \varepsilon D_1 + \varepsilon^2 D_2 + \cdots$$

$$\frac{d^2}{dt^2} = D_0^2 + 2\varepsilon D_0 D_1 + \varepsilon^2(2D_0 D_2 + D_1^2) + \cdots, \quad (5)$$

where derivatives $D_n = \partial/\partial T_n$ and $T_n = \varepsilon^n t$ correspond to different time scales.

We evaluate the general form of solution

$$X = x(T_0, T_1, \ldots; \varepsilon) \quad (6)$$

to the first and the second order of perturbation ε the solutions may be presented in the following forms:

- solution in the first order approximation:

$$x(t) \approx a \cos\left(\frac{1}{2}\Omega t + \psi\right), \quad (7)$$

where a and ψ satisfy the set of equations:

$$\dot{a} = \varepsilon\left(\frac{\alpha}{2}a - \frac{\beta}{8}a^3 - \frac{\mu}{2\Omega}a \sin(2\psi)\right) \quad (8)$$

$$a\dot{\psi} = \varepsilon\left(-\frac{\sigma_1}{\Omega}a + \frac{3\gamma}{4\Omega}a^3 - \frac{\mu}{2\Omega}a \cos(2\psi)\right) \quad (9)$$

- solution in the second order approximation:

$$x(t) \approx a \cos\left(\frac{1}{2}\Omega t + \psi\right) + \varepsilon\left[-\frac{\mu a}{4\Omega^2}\cos\left(\frac{3}{2}\Omega t + \psi\right) + a^3\left(\frac{\gamma}{8\Omega^2} + \frac{i\beta}{4\Omega}\right)\cos\left(\frac{3}{2}\Omega t + 3\psi\right)\right], \quad (10)$$

where a and ψ satisfy the set of equations:

$$\dot{a} = \varepsilon\left(\frac{\alpha}{2}a - \frac{1}{8}\beta a^3 - \frac{\mu}{2\Omega}a \sin(2\psi)\right) + \varepsilon^2\left(-\frac{3\alpha\gamma}{4\Omega^2}a^3 + \frac{11\beta\gamma}{64\Omega^2}a^5 + \frac{\beta\mu}{16\Omega^2}a^3 \cos(2\psi) + \frac{5\mu\gamma}{8\Omega^3}a^3 \sin 2\Psi\right) \quad (11)$$

$$a\dot{\psi} = \varepsilon\left(-\frac{\sigma_1}{\Omega}a + \frac{3\gamma}{4\Omega}a^3 - \frac{\mu}{2\Omega}a \cos(2\psi)\right) + \varepsilon^2\left[\left(-\frac{\sigma_1^2}{\Omega^3} - \frac{\alpha^2}{4\Omega} + \frac{3\mu^2}{8\Omega^3}\right)a \right.$$

$$\left. + \left(\frac{3\gamma\sigma_1}{2\Omega^3} + \frac{\alpha\beta}{4\Omega} - \frac{\gamma\mu}{4\Omega^3}\cos(2\psi) - \frac{\beta\mu}{8\Omega^2}\sin(2\psi)\right)a^3 + \left(-\frac{15\gamma^2}{32\Omega^3} - \frac{7\beta^2}{128\Omega}\right)a^5\right]. \quad (12)$$

Results (7–9) of the first order solution were obtained earlier by Huseyin and Rui [1992] and Rui and Huseyin [1992] so our principal result in this section is obtaining solution of the second order [Eqs. (10)–(12)]. Figure 1 show vibration amplitude plots versus frequency of parametric excitation. Lines were obtained as result of analytical

research (AR) in first order approximation of solution [Eqs. (8) and (9)].

Comparative points obtained during numerical simulation by means of Runge–Kutta–Gill algorithm (RKG) [Eq. (2)] are also presented and marked by full [Fig. 1(a)] or open [Fig. 1(b)] circles.
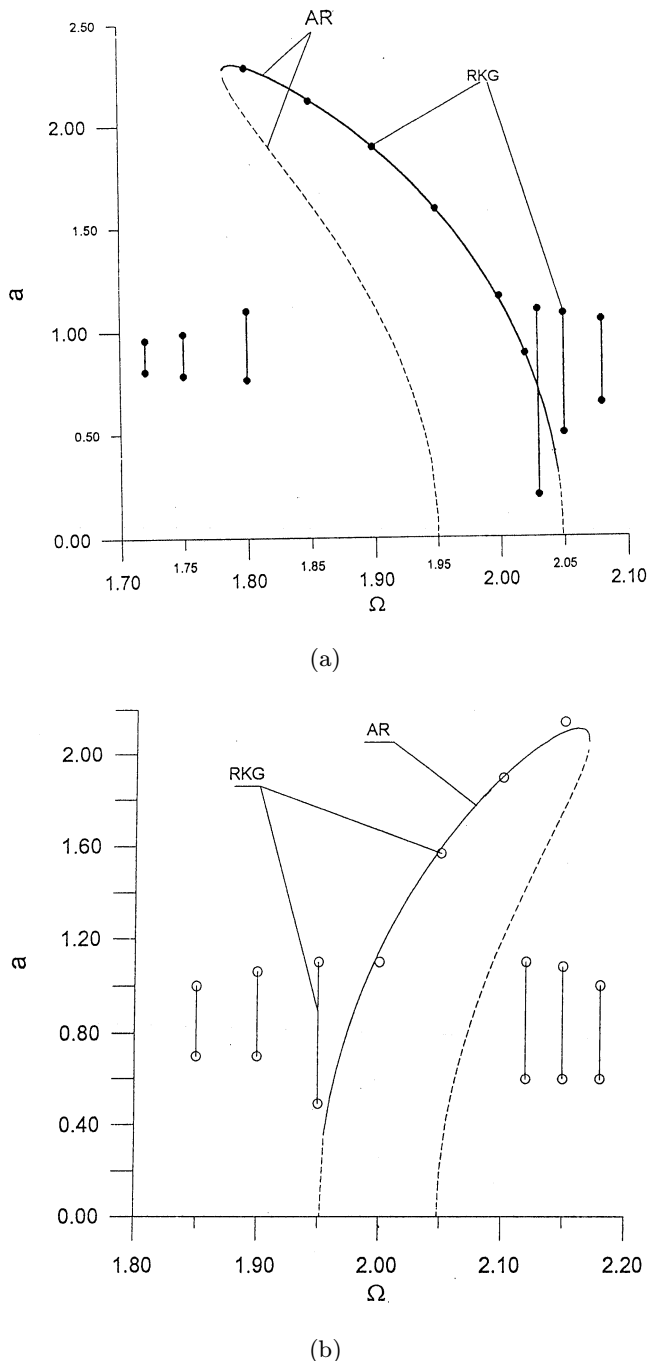
(a)

(b)

Fig. 1. Vibration amplitude a versus frequency of parametric excitation: (a) $\gamma = -1$ for soft characteristic, (b) $\gamma = 1$ for stiff one. Lines correspond to analytic results (AR) (full lines correspond to stable solutions whilst dashed lines to unstable ones respectively), circles to numerical ones (RKG).

In the middle of both pictures the synchronization area with mono frequency are visible. Outside these areas beats corresponding to quasi-periodic vibrations occur. System parameters used in the investigations [Eqs. (4) and Eqs. (8)–(10)] were following: $\alpha = 0.1$, $\beta = 0.5$, $\mu = 1.0$, $\varepsilon = 0.1$ $\delta = 1$. The

parameter γ was taken $\gamma = -1.0$ for Fig. 1(a) and $\gamma = 1.0$ for Fig. 1(b) respectively. These correspond to soft and stiff characteristics of the nonlinear force [Eq. (2)].

3. Solution Stability Analysis

To proceed the analysis of solution stability we disturb to the initial conditions. The disturbance δ is defined as the subtraction between disturbed and undisturbed solutions:

$$\Delta = \tilde{x} - x \qquad (13)$$

After applying Eq. (13) to Eq. (2) and subtraction the same but unperturbed equation [Eq. (2)] and linearization we get the following differential equation:

$$\ddot{\Delta} - \varepsilon(\alpha - \beta x^2)\dot{\Delta}$$
$$+ (1 + 2\beta\varepsilon x\dot{x} - \mu\varepsilon \cos \Omega\tau + 3\gamma\varepsilon x^2)\Delta = 0 \qquad (14)$$

On the base of Eq. (14) we has found the monodromy matrix and have examined stability of obtained solutions.

The eigenvalues of the monodromy matrices (Floquet multipliers) determine stability and unstability of solutions [Szabelski & Warmiński, 1995a]. Some exemplary values of Floquet multipliers for different values of parametric forcing frequency Ω and other values as in Fig. 1 are put in Table 1 for $\gamma = 1.0$ and in Table 2 for $\gamma = -1.0$.

The same sets of Floquet multipliers are presented in Fig. 2 for soft ($\gamma < 0$) and stiff ($\gamma > 0$) types of spring characteristics. Figures 2(a) and 2(b) show the unitary circles in the complex plane with the Floquet multipliers marked out. Figure 2(a) corresponds to Fig. 1(a) and Table 1 whilst Fig. 2(b) to Fig. 1(b) and Table 2 respectively.

Transition through this circle from outside to inside area corresponds to transition of an unstable solution into stable one. One can easily notice that point No. 8. (Table 1) and point No. 1 (Table 2) are situated outside the unitary circle in the complex plane [Figs. 2(a) and 2(b) respectively]. This means that for that chosen sets of system parameters solutions are unstable. The other points which lie inside the unitary circle indicate stable solutions.

Note that stable and unstable solutions are also marked in the amplitude plots (Fig. 1) where full lines correspond to stable solutions and dashed lines to unstable ones respectively.

Table 1.   Examples of Floquet multipliers which correspond to Fig. 2(a).

No.	Ω	x	$\dot{x}$	Multipliers	
1	1.785	1.71078	1.37049	-0.73236, 0.00000	-0.87956, 0.00000
2	1.800	1.52429	1.54262	-0.79670, -0.13130	-0.79670, 0.13130
3	1.850	1.05822	1.72714	-0.81010, -0.21590	-0.81010, 0.21590
4	1.900	0.67112	1.69528	-0.84640, -0.22600	-0.84640, 0.22600
5	1.950	0.33860	1.15092	-0.89490, -0.20480	-0.89490, 0.20480
6	2.000	0.07380	1.13380	-0.95230, -0.15300	-0.95230, 0.15300
7	2.020	-0.00040	0.88994	-0.97740, -0.11880	-0.97740, 0.11880
8	2.045	0.02885	0.32552	-1.01040, -0.04242	-1.01040, 0.04242

Table 2.   Examples of Floquet multipliers which correspond to Fig. 2(b).

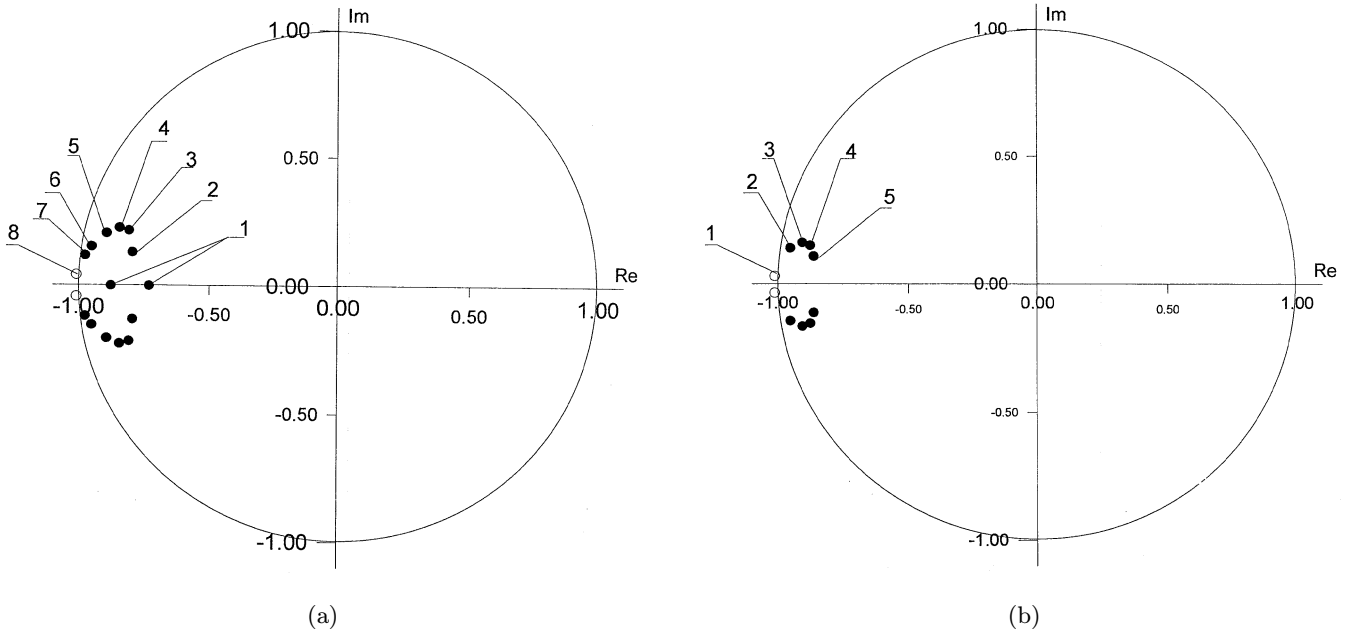| No.	Ω	x	$\dot{x}$	Multipliers	
1	1.953	0.22497	0.008	-1.013050, -0.032990	-1.013050, 0.032990
2	2.000	1.14540	-0.002	-0.954290, -0.142235	-0.954290, 0.142235
3	2.050	1.59320	0.013	-0.909116, -0.163160	-0.909116, 0.163160
4	2.100	1.90550	0.017	-0.878870, -0.152490	-0.878870, 0.152490
5	2.150	2.10650	0.055	-0.865090, -0.110320	-0.865090, 0.110320

Fig. 2.   Eigenvalues of monodromy matrices on the complex surface: (a) for $\gamma = -1$ soft characteristic, (b) $\gamma = 1$ for stiff one.

4. Chaotic Vibration of the System

As far as chaos investigations of this class of the system are concerned chaos was investigated for the similar vibrations model with van der Pol terms, nonlinearity of Duffing-type but an external excitation in the form [Ueda & Akamatsu, 1981; Steeb & Kunick, 1987; Kapitaniak & Steeb, 1990]:

$$\ddot{x} - (\alpha - \beta\dot{x}^2)\dot{x} + (\delta + \gamma x^2)x = B\,\cos(\omega t + \phi_0)\,. \quad (15)$$
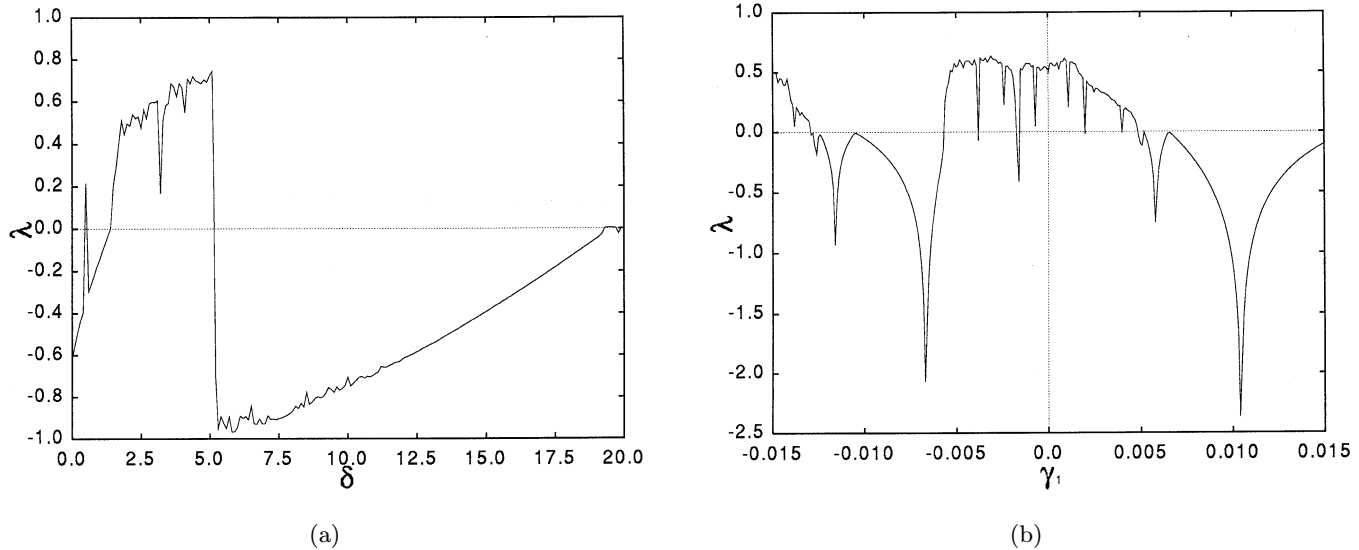
(a)

(b)

Fig. 3.   Lyapunov exponent λ as a function of $\delta - 3a$ ($\gamma_1 = 1$) and $\gamma_1 - 3b$ ($\delta = 1.9$); other parameters have following values: $\alpha_1 = 0.2$, $\beta_1 = 0.2$, $\mu_1 = 17$, $\Omega = 4$.

For that equation the scope of parameters, leading to chaos solutions, was determined. In articles [Ueda & Akamatsu, 1981; Steeb & Kunick, 1987], $\delta = 0$ was used. In papers of Kapitaniak and Steeb [1990], cases with $\delta \neq 0$ and $\gamma \neq 0$, for small γ ($\gamma \ll \delta$) were examined. In this paper we would like to provide the analogous analysis of Eq. (1) for stiff and soft case: $\gamma_1 > 0$ and $\gamma_1 < 0$ respectively.

Applying Wolf algorithm [Wolf *et al.*, 1988], maximal Lyapunov exponents [Eq. (1)] for the following set of parameters: $\alpha_1 = 0.2$, $\beta_1 = 0.2$, $\mu_1 = 17$, $\Omega = 4$, $\gamma_1 = 1$, as a function of the linear term coefficient [Eq. (1)] δ ($\delta \in [0, 20]$) [Fig. 3(a)] and for $\alpha_1 = 0.2$, $\beta_1 = 0.2$, $\mu_1 = 17$, $\Omega = 4$, $\delta = 1.9$ as a function of nonlinear cubic term coefficient [Eq. (1)] γ_1 ($\gamma_1 \in [-0.015, 0.015]$) have been found [Fig. 3(b)]. In our numerical simulations we assumed the initial conditions to be equal to $x_0 = 0.5$ and $\dot{x}_0 = 0.5$.

In Fig. 3(a) we can point out the interval of parameter values ($\delta \in [1.5, 5.1]$) for which exponent λ is positive. For δ values from that interval, the system behaves in a chaotic way. We have also investigated larger values of δ i.e. $\delta > 20$ but we have not found any positive values of λ (no chaotic solutions) for assumed other values of system parameters. Similarly in Fig. 3(b) we can recognize a number of intervals with positive λ. For such γ_1 values belonging to the intervals with positive λ the solutions of Eq. (1) should be chaotic. Moreover from

Fig. 3(b) one can see that chaotic solutions exist for both positive and negative γ_1. Our calculations for larger values of $|\gamma_1|$ ($|\gamma_1| > 0.015$) indicate that there other intervals of chaotic solutions parameters also exist.

Regular and Chaotic type of solution are connected with the appropriate Poincaré maps. Figures 4(a)–4(e) show Poincaré maps for chosen values of δ [other parameters are as in Fig. 4(b)]. In Figs. 4(a) ($\delta = 1.3$) and 4(d) ($\delta = 5.3$) system vibrations is synchronized. Attractors of this regular motions correspond to two [Fig. 4(a)] and one [Fig. 4(d)] points respectively. Figures 4(b) ($\delta = 1.7$) and 4(c) ($\delta = 5.0$) show strange attractors of chaotic motion. In these pictures one can see the evolution of shape of the strange attractor with increasing δ. At last for larger value of δ ($\delta = 20$), Fig. 4(e) presents the limit cycle attractor of quasi-periodic motion characteristic for self-excited systems. This is a regular motion with two nonrational frequencies.

For better clarity we present the examples of time histories for chosen values of δ: Fig. 5(a) for $\delta = 1.7$ and Fig. 5(b) for $\delta = 20$. Chaotic motion of system which occurs at $\delta = 1.7$ [the motion is characterized by positive value Lyapunov exponent Fig. 3(a) and the strange attractor Fig. 4(b)] has evidently nonperiodic time history while at $\delta = 20$ [the motion is characterized by nodal value of Lyapunov exponent Fig. 3(a) and the limit cycle attractor Fig. 4(e)] we see clearly regular motion with beats.
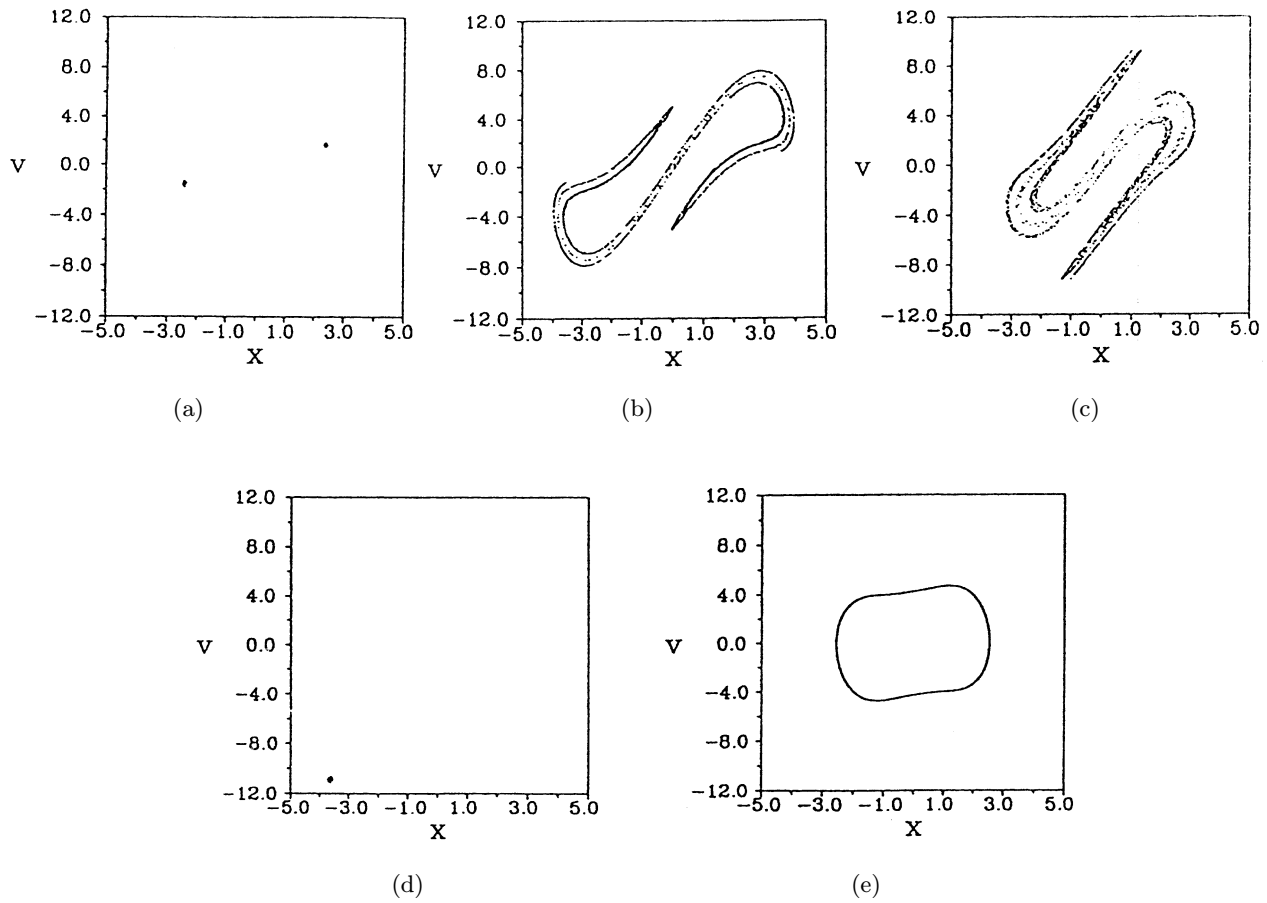
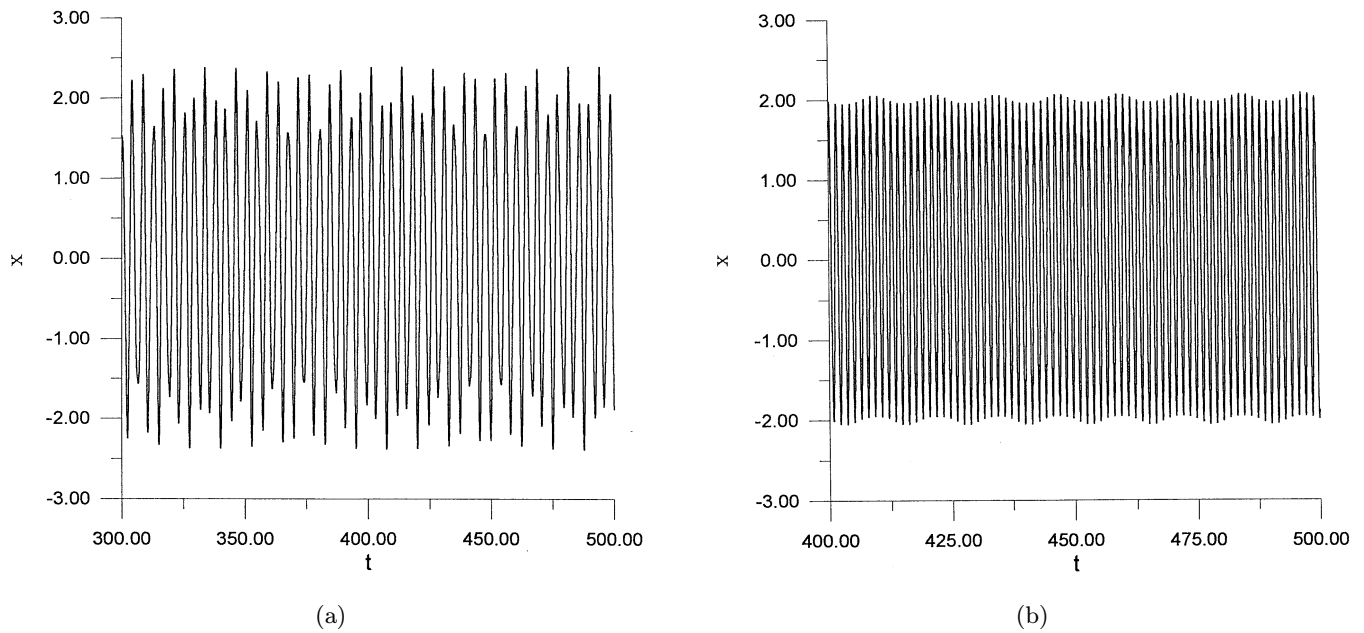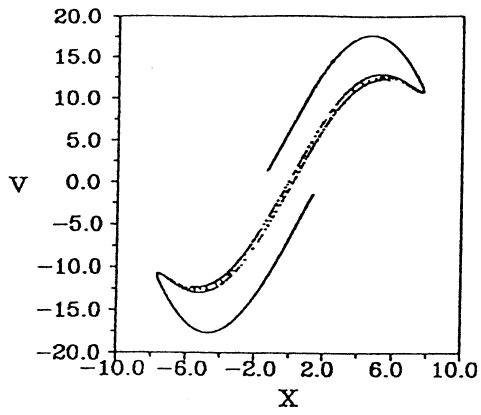Fig. 4.   Poincaré maps for different δ, other parameters as in Fig. 3(a).
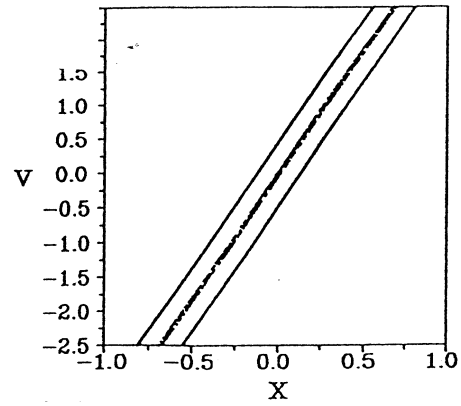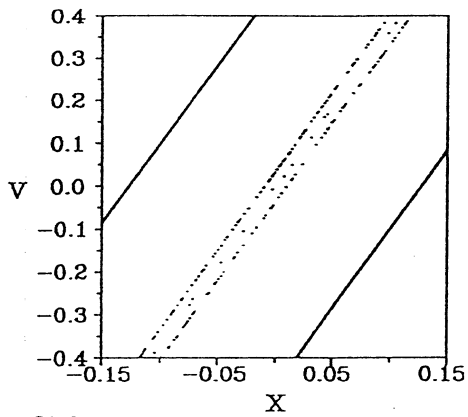

Fig. 5.   Time histories for two values of δ [$\delta = 1.7$ for Fig. 5(a) and $\delta = 20$ for Fig. 5(b)] other parameters as in Fig. 3(a).
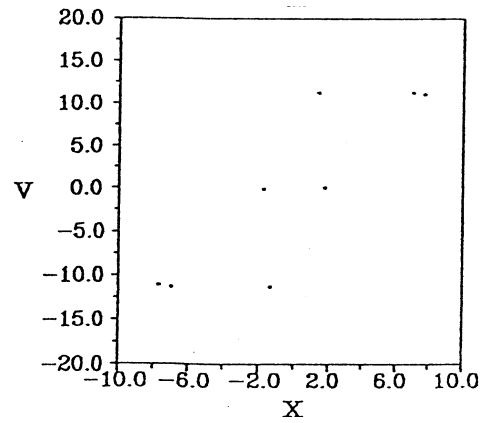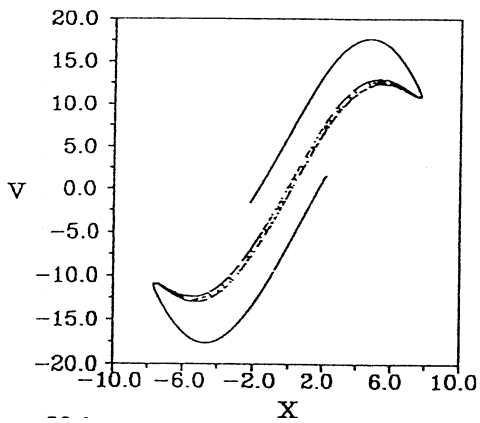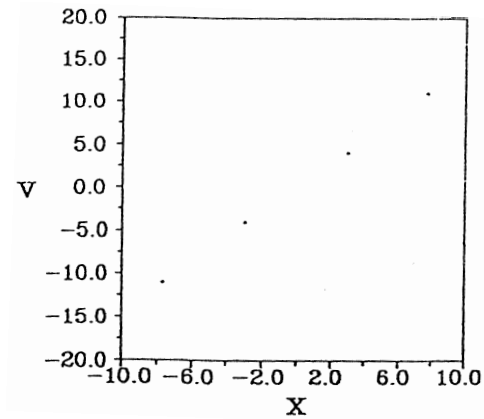
Fig. 6. Poincaré maps for different γ_1, other parameters as in Fig. 3(b).
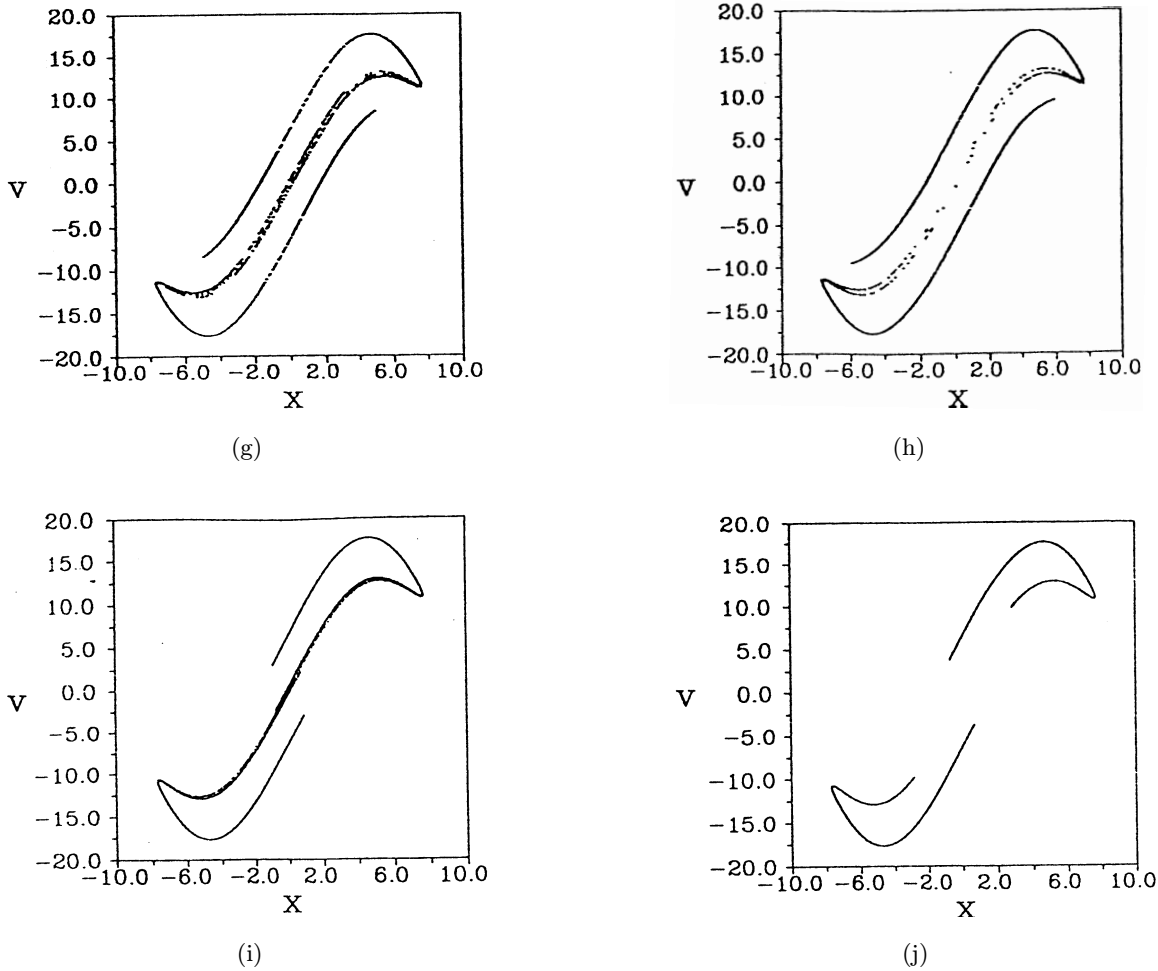
(g)

(h)

(i)

(j)

Fig. 6.   (*Continued*)

On the other hand Figs. 6(a)–6(h) show Poincaré maps for chosen values of γ_1 and the same δ. For Figs. 6(a)–6(c) γ_1 takes the same zero value; $\gamma = -0.0016$ for Fig. 6(d), $\gamma_1 = -0.0031$, for Fig. 6(e), $\gamma_1 = -0.0061$, for Fig. 6(f), $\gamma_1 = -0.015$, for Fig. 6(g), $\gamma_1 = -0.02$ for Fig. 6(h). Starting from $\gamma_1 = 0$ we recognize the strange attractor [Fig. 6(a)]. Characteristic three lines splitting in different scales provide the evidence of the fractal structure of this attractor [Figs. 6(b) and 6(c)]. Going with parameter γ_1 to smaller negative values we have detected other chaotic [Fig. 6(e)] and regular attractors [Figs. 6(d) and 6(f)]. They correspond to positive and negative values of Lyapunov exponent λ (Fig. 3). Even for smaller negative values of $\gamma_1 = -0.015$ [Fig. 6(g)], $\gamma_1 = -0.02$ [Fig. 6(h)] we have found also strange attractors of the similar structure. Figure 6(i) corresponds to positive values of $\gamma_1 = 0.0015$. Note that both negative and

positive values of the nonlinear term coefficient γ_1 lead to the similar global structures of strange attractor. One of the differences is however in the line on border of the global attractor structure (Fig. 6) which is shorter for positive γ_1 and longer for negative one.

We also have checked that among the set of γ_1 parameters which lead to a chaotic solution with positive Lyapunov exponent [Fig. 3(b)] there are also some short intervals of γ_1 with a regular solution. For one of such values $\gamma_1 = 0.0021$ we have plotted the Poincaré map [Fig. 6(j)]. This plot indicates that the motion type for this γ_1 is quasiperiodic with the limit cycle.

Figures 7(a)–7(e) presents phase portraits which are plotted for examined earlier sets of system parameter values. Starting from the same, examined earlier initial conditions $x_0 = 0.5$ and $\dot{x}_0 = v_0 = 0.5$ phase portraits are plotted using
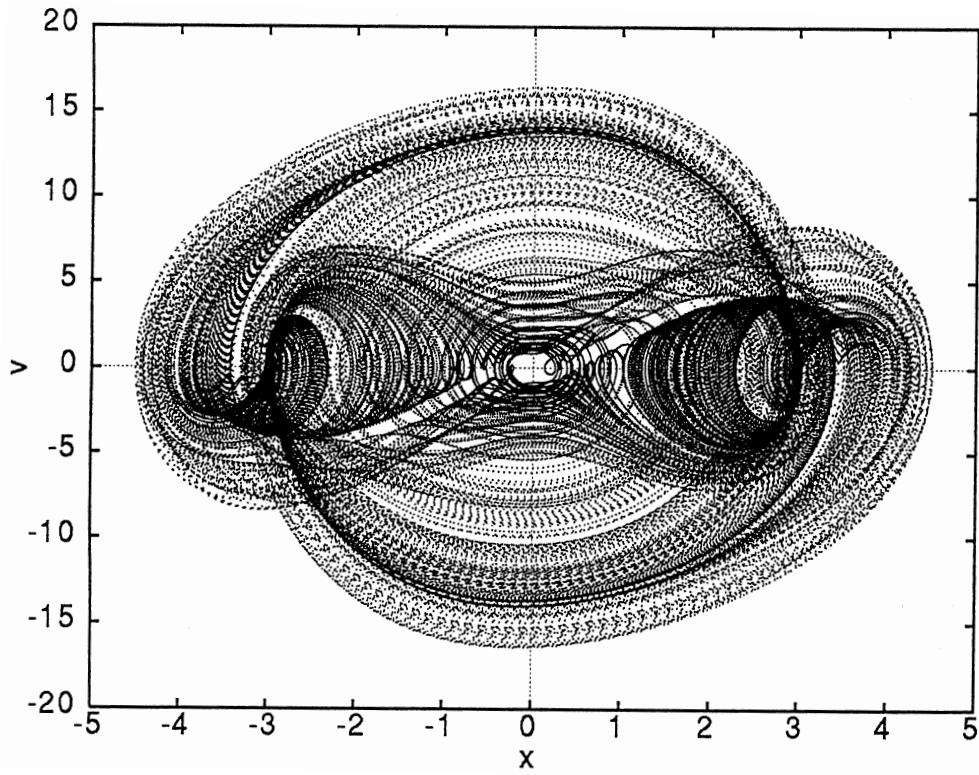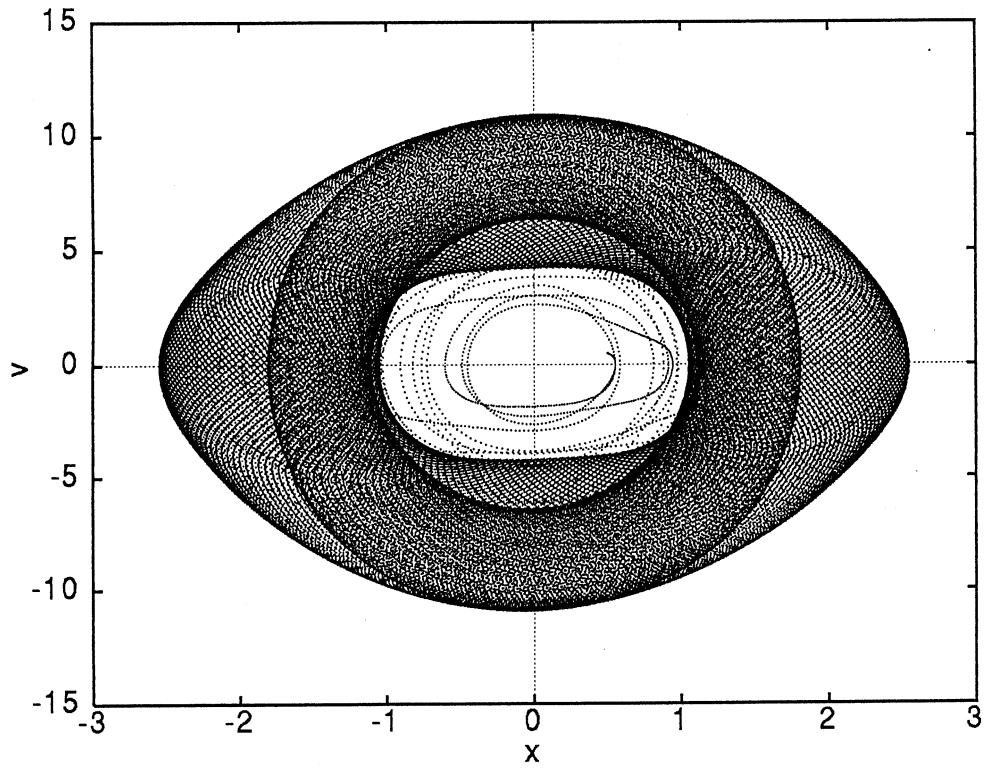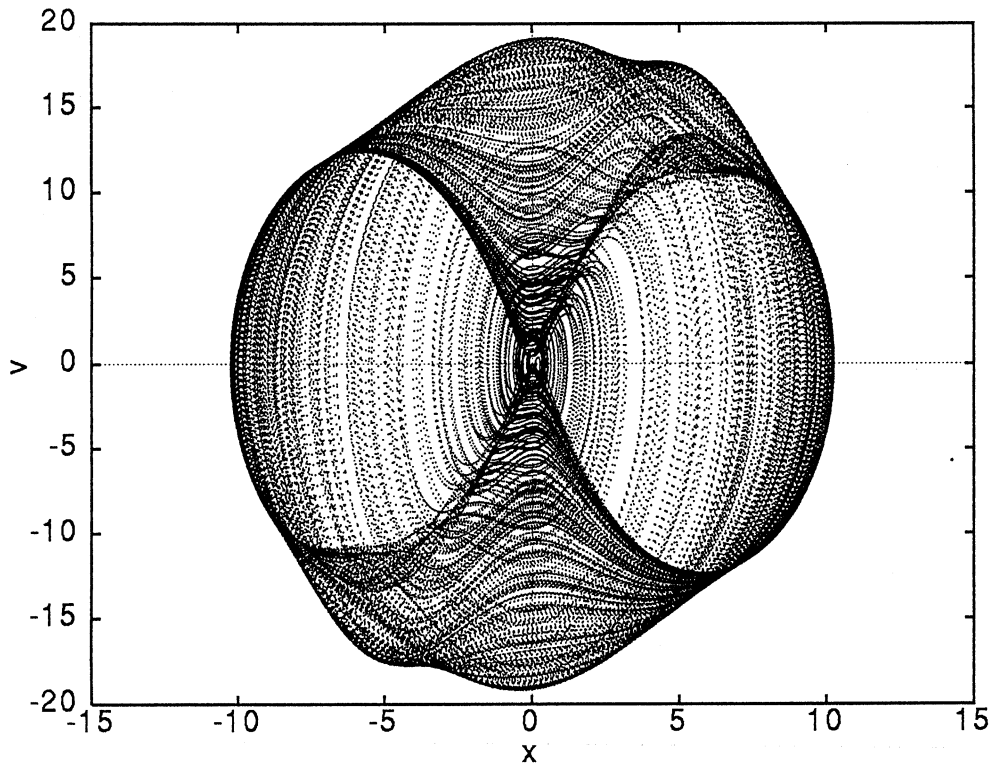
(a)
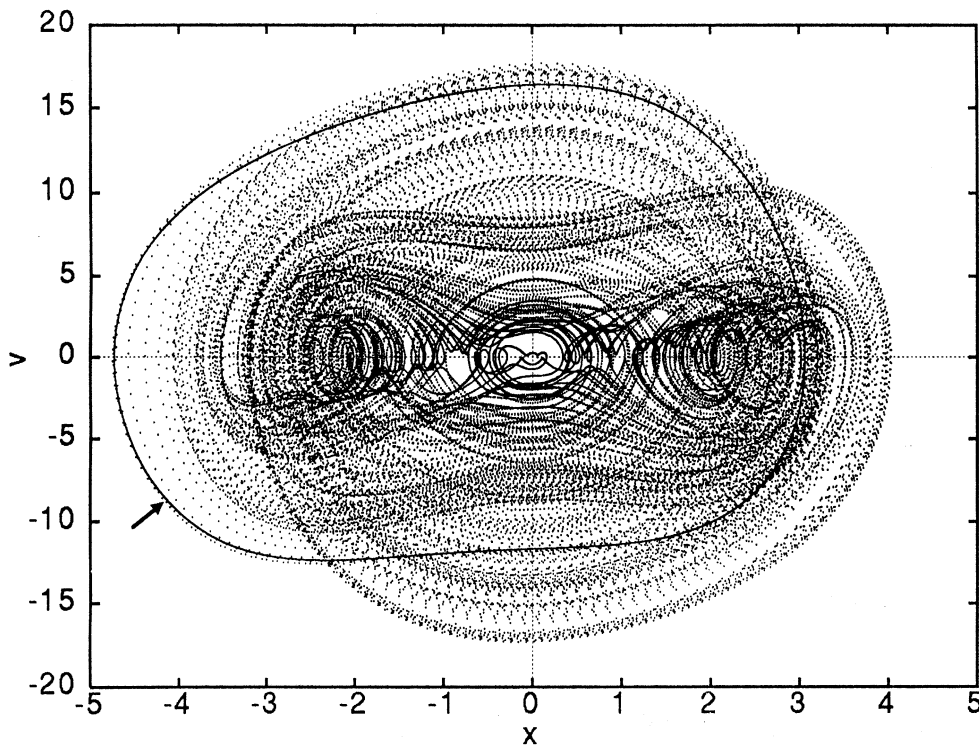
(b)

Fig. 7. Phase portraits for some sets of parameter values of γ_1 and δ [$\delta = 1$, $\gamma_1 = 1.7$ for Fig. 7(a); $\delta = 5.3$, $\gamma_1 = 1$ for Fig. 7(b); $\delta = 20.0$, $\gamma_1 = 1$ for Fig. 7(c); $\delta = 1.9$, $\gamma_1 = 0.0015$ for Fig. 7(d); $\delta = 1.9$, $\gamma_1 = 0.0021$ for Fig. 7(e)].
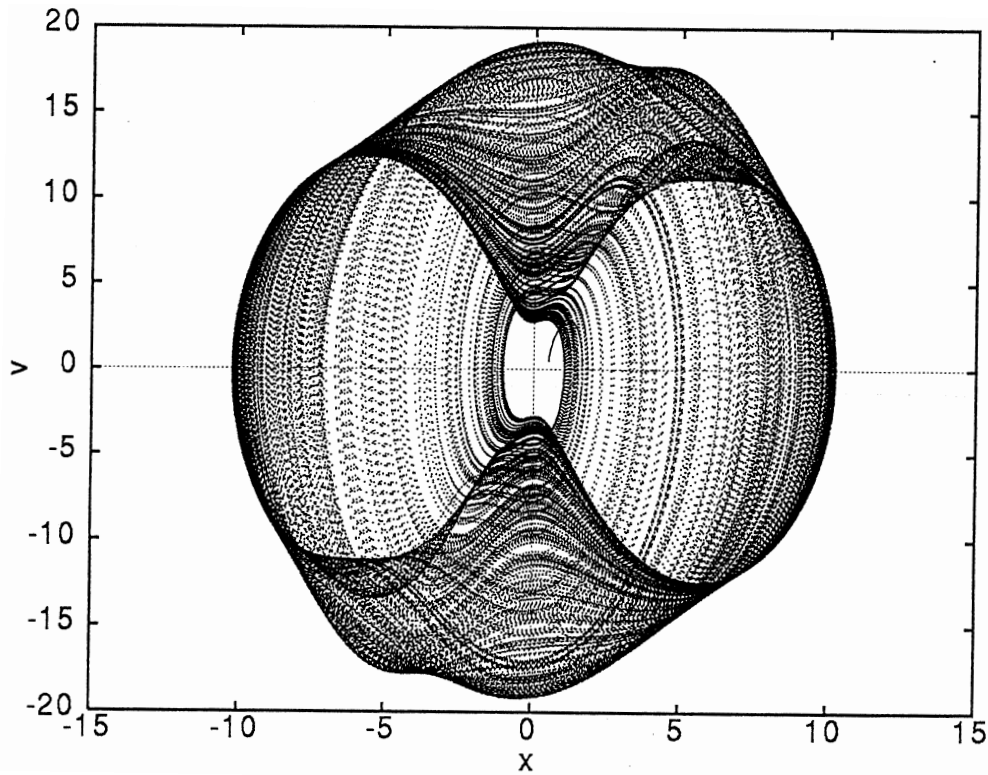
(c)

(d)

Fig. 7.   (*Continued*)

(e)

Fig. 7.   (*Continued*)

dots for a long time interval. In Fig. 7(a) ($\delta = 1.7$, $\gamma_1 = 1$) we see phase portrait of the chaotic motion. It corresponds to the appropriate strange attractor in Poincaré map [Fig. 4(b)] and chaotic time history plotted in Fig. 5(a). Figure 7(b) represents regular, periodic motion phase portrait for $\delta = 5.3$ and $\gamma_1 = 1$. Note that the steady state which is connected with the closed line marked by an arrow in reached after rather long time. An intermediate state and time of approaching to the steady state depend on the initial conditions. This phase portrait corresponds to plotted earlier the singular point regular attractor of a synchronized motion in Poincaré map [Fig. 4(d)]. For larger value of δ parameter the motion of system evaluate to quasi-periodic vibrations. Figure 7(c) shows the example of this type of motion phase portrait [here δ has been taken to be equal to 20 and $\gamma_1 = 1$ as in Figs. 4(e) and 5(b)]. The regular pattern of this attractor well visible. Another types of phase portraits shown in Figs. 7(d) and 7(e) correspond also to two examples of examined earlier cases: $\gamma_1 = 0.0015$ and $\gamma_1 = 0.0021$ ($\delta = 1.9$). These two values of γ_1 correspond to two types of motion which are quite

different according to Poincaré maps plotted in Figs. 6(i) and 6(j). They describe chaotic and quasi-periodic attractor respectively. However the vase-like phase portraits of these motions are very similar to each other. The difference which one can notice is that the chaotic motion phase portrait is full in the middle while quasi-periodic motion ones is empty. This may be connected with the type of self-similarity of the strange attractor Figs. 6(a)–6(c). One can see in these pictures [Figs. 6(a)–6(c)] that self-similarity, the fundamental structure feature of strange attractors is not applicable to the whole attractor but only the middle part of it. The lack of middle structure in Fig. 7(e) may mean then the lack of self-similarity. This can cause the transition of system from chaotic motion to regular one.

5.   Summary and Conclusions

Considering existing and stability of differential equation solutions, the interaction effects of self-excited and parametric vibrations were determined. It was found that vibrations synchronization in

particular frequency interval of parametric excitation took place. Analytic investigation was carried out under certain simplified assumptions and their verification was obtained using numerical simulation. Applying Lyapunov exponents method, chaotic vibrations were found for particular parameters of the system. In particular we investigated the system answer to change of linear and nonlinear force term coefficients. We have also examined the evolution of the strange attractors plotting Poincaré maps and phase portraits of the model numerical simulations for various system parameters. All calculations have been done for the assumed initial conditions so analysis on possible coexistence of different attractors for different initial conditions we left to a future paper.

Acknowledgments

References

Huseyin, K. & Rui, L. [1992] "A perturbation method for the analysis of vibrations and bifurcations associated with non-autonomous systems I. Nonresonance case," *Int. J. Nonlin. Mech.* **27**, 203–217.

Kapitaniak, T. & Steeb, W.-H. [1990] "Transition to chaos in a generalized van der Pol's equation," *J. Sound Vib.* **143**, 167–170.

Parker, T. S. & Chua, L. O. [1989] *Practical Numerical Algorithms for Chaotic System* (Springer-Verlag, NY).

Parlitz, U. & Lauterborn, W. [1987] "Period-doubling cascades and devil's staircase of the driven van der Pol oscillator," *Phys. Rev.* **A36**, 1428–1434.

Rui, L. & Huseyin, K. [1992] "A perturbation method for the analysis of vibrations and bifurcations associated with non-autonomous systems II. Resonance case," *Int. J. Nonlin. Mech.* **27**, 219–232.

Steeb, W.-H. & Kunick, A. [1987] "Chaos in system with limit cycle," *Int. J. Nonlin. Mech.* **22**, 349–361.

Szabelski, K. [1984] "Drgania układu samowzbudnego z wymuszeniem parametrycznym i nieliniową sprężystością," *Mechanika Teoretyczna i Stosowana* **22**, 171–183 (in Polish).

Szabelski, K., Litak, G., Warmiński, J. & Spuz-Szpos, G. [1996] "Vibration synchronization and chaos in the parametrically self-excited system with non-linear elasticity," in *Proc. EUROMECH — 2nd European Nonlinear Oscillation Conf.*, Prague, Sep. 9–13, pp. 435–438.

Szabelski, K. & Warmiński, J. [1995a] "Self-excited system vibrations with parametric and external excitations," *J. Sound Vib.* **187**, 595–607.

Szabelski, K. & Warmiński, J. [1995b] "Parametric self-excited non-linear system vibrations analysis with internal excitation," *Int. J. Nonlin. Mech.* **30**, 179–189.

Szabelski, K. [1991] "The vibrations of self-excited system with parametric excitation and non-symmetric elasticity characteristic," *Mechanika Teoretyczna i Stosowana* **29**, 57–81.

Ueda, Y. & Akamatsu, N. [1981] "Chaotically transitional phenomena in the forced negative-resistance oscillator," *IEEE Trans. Circuits Syst.* **CAS-28**, 217–224.

van der Pol, B. [1926] "On relaxation-oscillations," *Phil. Mag.* **2**, 978–992.

van der Pol, B. & van der Mark, J. [1928] "The heartbeat considered as a relaxation oscillation and an electrical model of the heart," *Phil. Mag. Suppl.* **6**, 763–775.

von Hertzen, R. & Kongas, O. [1996] "Nonlinear dynamics of cardiac action potential oscillations," in *Proc. EUROMECH — 2nd European Nonlinear Oscillation Conf.*, Prague, Sep. 9–13, pp. 23–32.

Wolf, A., Swift, J. B., Swinney, H. L. & Vasano, J. A. [1988] "Determining Lyapunov exponents from a time series," *Physica* **D16**, 285–317.